Discussing the electrical phenomenon of sharp points power through mechanical modeling and video analysis

R. S. Dutra *, J. Ataliba, A. R. Pimenta, R. P. Freitas,
V. S. Felix, E. A. S. Gonçalves, D. S. R. Ferreira, L. O. Pereira,

Laboratório de Instrumentação e Simulação Computacional,
Instituto Federal do Rio de Janeiro, 26600-000, Paracambi-RJ, Brasil

March 22, 2022

Abstract

This paper performs a semi-quantitative and low-cost experiment, combining video analysis technique and mechanical modeling, to discuss the known electrical phenomenon of the power of sharp points in undergraduate physics laboratory classes. To this end, we perform a video analysis of the spin movement of an electric whirl on the top of an electrostatic generator. When considering a simple model, the kinematic and dynamic analyses are used to obtain a superior bound for the modulus of the electric charge propelled from the air, creating the electric wind due to the corona effect. Analytical results for the mechanical modeling are validated using *SolidWorks* simulations and the electronic microscopy experimental technique.

1 Introduction

The use of information and communication technologies (ICTs) in science teaching has inserted students and teachers in a high-quality scenario of

*e-mail: rafael.dutra@ifrj.edu.br

teaching and learning process [1, 2]. In this way, ICTs can motivate and inspire students through activities that promote cooperation between colleagues in a class. An active learning process involving the solution of concrete problems, when used joint, for example, with a contemporary educational approach based on Science, Technology, Engineering, Arts and Mathematics (STEAM) [3, 4, 5]. In particular, applications of ICTs in physics teaching currently involve two essential fronts, the use of simulations using computers and electronic devices, like smartphones, tablets, and Arduino, together with experiments to discuss important physical concepts [6, 7, 8]. Computers and software make physics classes richer, discussing ideas using simulations on the screen computer, like a computational experiment. From the evaluative educational process point of view, the use of simulations has also been used to evaluate the performance of the learning process of students [9, 11]. In the last ten years, with the crescent use of smartphones, the video analysis technique has been a powerful tool the physics education community uses to promote more attractive physics activities at schools and universities. Visualization and discussion of the physics aspects never seen before at the laboratory of basic physics classes, in a simple way, and, also, when used jointly with low-cost materials [10, 12, 13]. The video analysis technique has the power to increase the number of the experimental points over a given experimental realization in a simple way, allowing the study of several movements in one, two, or three dimensions. The use of mathematical modeling allows to quantify instantaneous kinematics and dynamics quantities [14, 15, 16, 17].

In this paper, we present a simple low-cost experiment, which combines mechanical modeling and video analysis techniques by using the free software *Tracker*[1]. We discuss in a semi-quantitative way the well-known electric phenomenon discussed during introductory physics courses, namely *power of sharp points*, present in metallic materials [18]. The experiment consists of recording the spin motion of an electric whirl [19], coupled on the top of an electrostatic generator, using a simple smartphone camera. The movement is induced by the charges accumulated at the sharp points of the metallic arms. The large electric fields created around the sharp points, which are bigger than air dielectric strength, propel the electrons attached in the air, making a small local flux of the electrons at the same time (electric wind) through the corona effect [20]. Due to Newton's third law, the electric wind

[1]https://physlets.org/tracker/

reacts exercising a force into the sharp points, generating a torque around the center of mass of the electric whirl as depicted in figure 1(d). Using video analysis, we track the circular motion of the sharp point to obtain the angular acceleration by kinematic analyses. Finally, we use a simple model to estimate a superior bound value for the charge propelled from the air due to the large electric field created around sharp points. Through the connection between kinematic and dynamic analysis, we first show how to model the inertia moment of the electric whirl in terms of its mass and lengths. During the procedures, *SolidWorks* simulations and the electronic microscopy experimental technique, not available in most classroom setting, are just used to validate our findings, not being necessary to use them.

Section 2 presents the methodology that allows connecting kinematic and dynamic of the spin motion using video analysis. After, in section 3, we show how to model the inertia moment of the electric whirl, which is important to describe the system's dynamic, separating it in terms of known geometric solids. In section 4 the results are presented, discussed, and finalized the conclusions in section 5.

2 Methodology

We have used a smartphone with a frame rate of $30fps$, to record the movement of an electric whirl placed on the top of an electrostatic generator, as depicted in figure 1(c). This motion is induced by the electric force F_e, represented by the red arrows at figure 1(d), into electric charges concentrated on the sharp points of whirl arms. The electric forces due to the electric wind acting on each one of the sharp points generate a resultant torque τ on the electric whirl, and consequently a rotational movement around its center of mass. We apply the video analysis technique to study the kinematic associated with the circular trajectory followed by the sharp points, using the free software *Tracker*. The figure 1(d) shows a periodic behavior for the graphics associated with the cartesian coordinates $x(t)$ and $y(t)$ of a given sharp point as a function of time, due to the projection of the circular motion along xy plane in terms of cosine and sine functions. The period of the circular movement decay over time, as expressed in terms of reducing the distance between two maxima or minima of the graphics, as a function of time. This behavior is a consequence of the angular acceleration α that arises due to the torque exercised by the electric wind, resulting in a growing angular velocity

$\omega(t)$ and a consequent reduction of the period T as a function of the number of turns n, such that, $2\pi n = \int_0^{nT} \omega(t)\, dt$. We can exemplify considering a motion with an angular acceleration constant, such that $\omega = \omega_0 + \alpha\, t$, and the period of the circular motion as a function of the number of turns n is given $T_n = 2\sqrt{\pi/\alpha\, n}$. The electric whirl initially in rest $\omega_0 = 0$ is considered, and in this case, the period is inversely proportional to the square root of the number of turns. From the kinematic analysis, it is possible to obtain the angular acceleration, and, consequently, the electric force acting on each one of the four sharp points, by applying Newton's second law for the dynamic of rotation to the electric whirl $\tau = I_z\alpha$, considering it as a rigid body:

$$4F_e(L + a) = I_z\alpha, \tag{1}$$

being I_z the inertia moment in relation to the rotational axis, defined along the z direction, and L the major length of the arm as depicted at figure 1(b) and a the radius cavity of the core as shown at figures 3(a) and (b). To obtain the electric force, in the next section, the modeling of the inertia moment I_z of the electric whirl will be considered in terms of its mass, geometric lengths, and material properties, validating it via computational simulation using the *SolidWorks* software.

3 Inertia moment modeling

In order to construct an analytical model describing the inertia moment of an electric whirl (depicted in figure 1(a)) around its rotation axis, the arms from the core have been separated, as shown in figure 1(b), and using a balance to find $m_{arm} = 0.9\, g$ and $m_c = 3.1\, g$, respectively, for the mass of each arm and core. The metallic core geometry modeling via *SolidWorks*, with all details, nonuniform and lateral cavities, and lengths, are shown in figure 2. The core scheme shown in figure 3(a) have been modeled, analytically, separating it into three simple homogeneous and regular geometric solids: two cylinders, ① and ③, and a truncated cone ②. The core also has an inside cylindrical cavity with radius $a = 0.24\, cm$, neglecting the lateral and nonuniform cavities. Therefore, the analytical modeling for the metallic core, represented in figure 3(a), is an approximation of the geometry shown in figure 2.

The rest of the geometrical lengths shown in figure 1(a) are summarized at the caption of figure 3(a). Aiming to calculate the inertia moment of

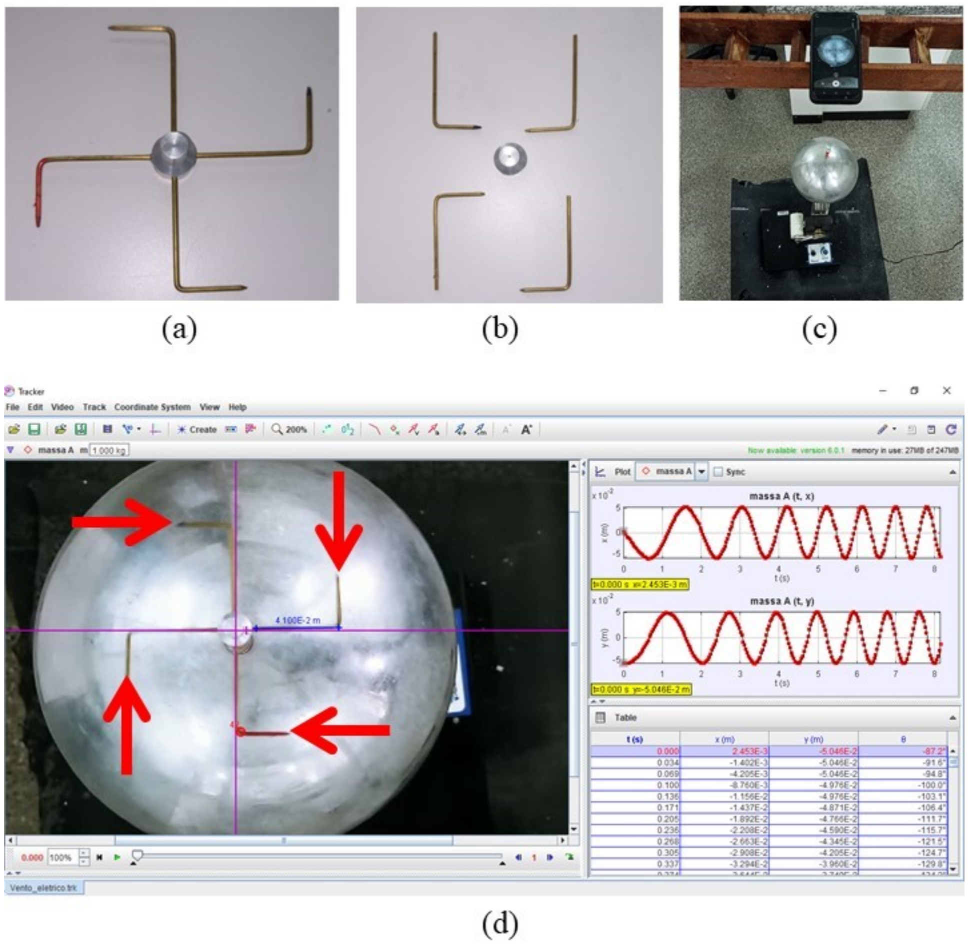

Figure 1: Experimental apparatus. (a) Electric whirl fabricated by brazilian company Azeheb of instruments for physics didactic laboratories. (b) Electric whirl separated in its different metallic parts: core + 4 arms. (c) Smartphone recording the rotation movement of electric whirl on the top of the electrostatic generator. (d) Video analysis process result using the *Tracker* software.

the core in relation to the rotation axis, we apply the respective formulas, summarized in table 1, for each one of the geometries ①, ②, and ③. The superposition principle has been applied to find the inertia moment of the core. The inertia moment of each one of three parts was superposed, and

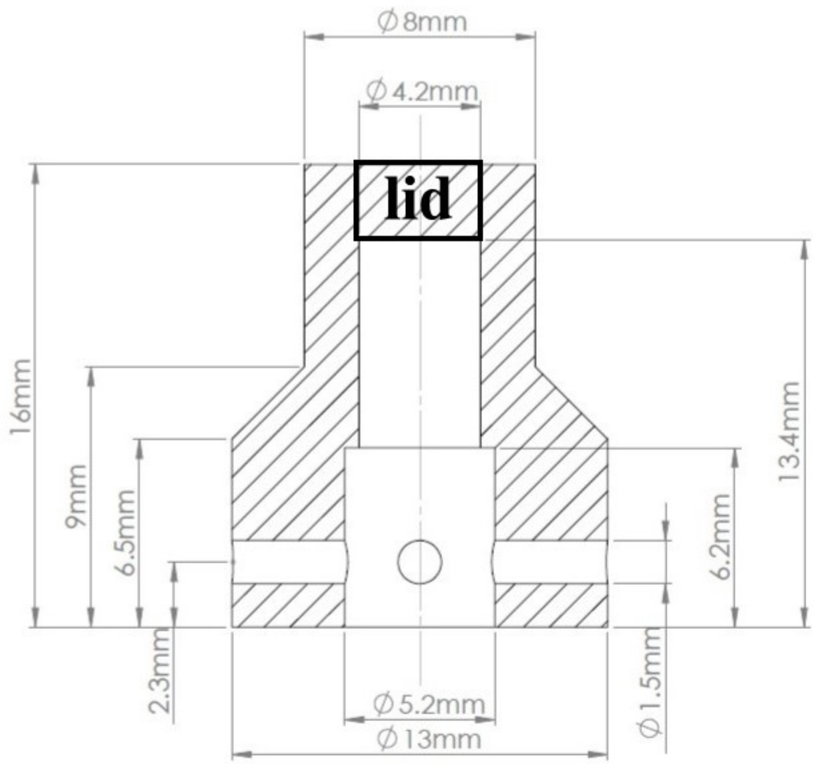

Figure 2: Modelling the metallic core geometry using the *SolidWorks* software.

subtracted the inertia moment of a cylinder of radius a, using formulas shown in table 1, to describe the effect of the cavity inside the core. The inertia moment associated with a truncated cone has been obtained using the inertia moment formula to a complete cone and, again, applying the superposition principle, considering the truncated cone as a part of a given cone. Therefore, the core's inertia moment, in terms of its mass and geometric parameters, can be modeled analytically by the following formula:

$$I_{z,c} = \underbrace{\frac{\pi\rho_c}{2}(r^4 - a^4)h}_{①} + \underbrace{\frac{\pi H'\rho_c}{10}\left(\frac{R^5 - r^5}{R - r}\right) - \frac{\pi H'\rho_c a^4}{2}}_{②}$$

Inertia moment	
cylinder	$\frac{\pi\rho\ell\tilde{R}^4}{2}$
cone	$\frac{\pi\rho\ell\tilde{R}^4}{10}$

Table 1: Inertia moment formulas for homogeneous cylinder and cone of density ρ, with height ℓ and radius $\tilde{R}$ [21].

$$+\underbrace{\frac{\pi\rho_c}{2}(R^4-a^4)H}_{③}+\underbrace{\frac{\pi\rho_c}{2}a^4h'}_{\text{lid}}, \tag{2}$$

with

$$\rho_c=\frac{3m_c(R-r)}{\pi H'[R^3-r^3-3(R-r)a^2]+3\pi(R-r)[(r^2-a^2)h+(R^2-a^2)H]+3(R-r)\pi a^2h'} \tag{3}$$

being the specific mass of the core. The thickness of lid that closes the top of the metallic core, with radius $a=0.24\ \ cm$, not specified in figure 3(a), is given by $h'=16-13.4=0.26\,cm$, according to figure 2, taken into account in the inertia moment of the core. On the equation 2 we specify the contribution to the inertia moment of the core due each one of the parts ①, ②, ③, and lid, discounting the contribution of internal cavity.

To calculate the inertia moment of the arms, we separate them into two parts, where each one have been treated in terms of a constant linear density of mass, neglecting its thickness. The first one has length L, parallel to the x axis with the left extremity of a distance a from the z rotation axis, as shown in figure 3(b), and the other is located along y axis with length l. Considering the arms homogeneous, where consequently the mass of each part is proportional to its lengths, and applying definition $I_z=\int r^2dm$, being r the distance between a given mass element dm in relation to the rotation axis, we obtain the following expression modeling the resultant inertia moment due to the four arms that compose the electric whirl

$$I_{z,arms}=\frac{4}{3}\frac{m_{arm}}{L+l}[L^3+l^3-a^3+3l(L+l)^2], \tag{4}$$

and therefore, the inertia moment of the electric whirl is given $I_{z,e}=I_{z,c}+I_{z,arms}$. The values of the arm lengths L and l are summarized in the caption of figure 3(b). To validate the analytical model, we simulate the inertia moment of the electric whirl computationally by using the *SolidWorks* software, as shown in figure 3(c). In this case, the input parameters are the geometric lengths of the system and the specific masses of the materials that compose the electric whirl. Visually the core and the arms are composed of different materials, and they have been characterized using an energy dispersive spectroscopy (EDS) detector attached to scanning electron microscopes (SEM), as will be discussed in the next section.

4 Results and discussion

The result obtained for the fitting of the sharp point angular position θ as a function of time t, using the parabolic model $\theta = At^2 + Bt + C$ (figure 4(a)), indicates that the torque produced by the electric forces acting on each one of the arms, have a constant behavior along the time and therefore the electric whirl performs a rotation motion, at a clockwise sense, with a constant angular acceleration $\alpha = 2A = -0.736 \pm 0.002\, rad/s^2$, with $A = -0.368 \pm 0.001\, rad/s^2$, $\omega_0 = B = -2.64 \pm 0.01 rad/s$ (initial angular velocity) and $\theta_0 = C = -1.20 \pm 0.02\, rad$ (initial angular position), obtained by the fitting.

Substituting the numerical values for masses and lengths into equations 2 and 4, we obtain, by analytical modeling, the value $I_{z,e} = 37.53\, g.cm^2$ for the inertia moment of the electric whirl. To validate the analytical result for the inertia moment, we have used *SolidWorks* as shown in figure 4(d). In this case, the characteristic lengths of the specific masses of the materials that compose each part of the system (arms and core) must be considered input parameters. Energy dispersive spectroscopy technique [22] has been used to characterize the materials of the arms and core. The spectra outputs obtained, as shown at figures 4(b) and 4(c), give the composition of brass alloy [23], for the arm, with 33% of Zn and 66% of Cu, and 100% of Al for the core. The specific masses associated to the last characterization, $\rho_{all} = 8.55\, g/cm^3$ (brass alloy) and $\rho_{Al} = 2.7\, g/cm^3$ (aluminum), respectively the materials of the arms and core, have been used as input parameters in computational simulations. The inertia moment calculated agrees analytically with the the result obtained from the *SolidWorks* modelling, $I_{z,s} = 39.55\, g.cm^2$, as highlighted in figure 4(d), with a relative percentual error of $(39.55 - 37.53) \times 100\%/39.55 \approx 5\%$, validating the analytical result. The most significant contribution to the inertia moment of the electric whirl comes from the arms, being $I_{z,arms} = 36.9\, g.cm^2$. Therefore the under-

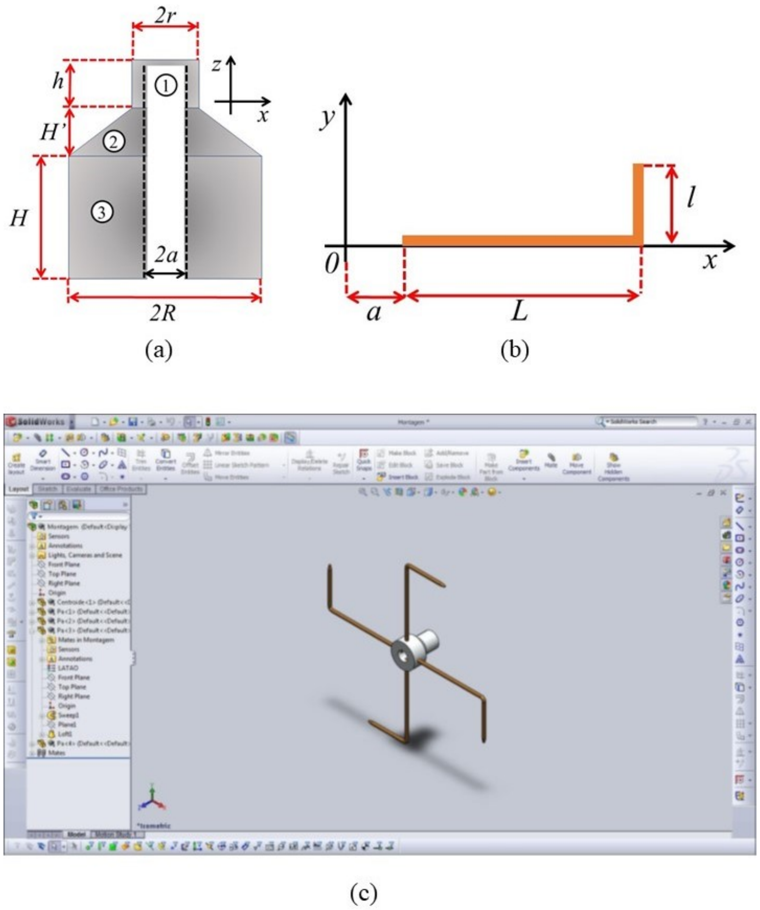

Figure 3: Modelling the geometry of the electric whirl. (a) Core modelled in terms of truncated cone between two cylinders, with lengths given by $H = 0.65\,cm$, $H' = 0.25\,cm$, $h = 0.7\,cm$, $r = 0.4\,cm$, $a = 0.26\,cm$ and $R = 0.65\,cm$. (b) Arms with lengths $L = 4\,cm$ and $l = 2.1\,cm$. (c) *SolidWorks* simulation.

estimated analytical value found (5% smaller than the one found by using *SolidWorks*), can be addressed to the way how the inertia moment of arms has been modeled in equation 4, i.e., in terms of a linear density of mass rather than a volume density, neglecting its thickness along the length. The same agreement, between analytical and experimental results, has been found for the specific mass of the core $\rho_c = 2.69\, g/cm^3$, obtained from equation 3. This result fully agrees with the input parameter ($\rho_{Al} = 2.7\, g/cm^3$) used to perform the simulations, which was obtained through the experimental procedure of the electronic microscopy.

In the end, the force due to electric wind acting on each sharp point of the whirl arms has been estimated, neglecting the friction forces acting on the system. By the substitution of the modulus of the angular acceleration $\alpha = 0.74\, rad/s^2$ (obtained from video analysis process) and the analytical result for inertia moment $I_{z,e} = 37.53\, g.cm^2$, into equation 1, we obtain $F_e = 1.6 \times 10^{-5}\, N$. We use the last value obtained to estimate a superior bound for the modulus of the electric charge q on each instant of time. This charge is propelled from the air due to the large electric field created by each of the four electrically charged sharp points of the arms, considering a simple approach in which electric charges are continuously propelled from the air. The modulus of the electric field generated by each charged sharp point must be bigger than the dielectric strength of the air to create the corona effect, that is, $E > 3 \times 10^6\, V/m$ [18]. By knowing that the electric force that acts on electrons attached in air molecules is given by $F_e = qE$, we estimate the experimental interval $0 < q_{exp} < 5.4\, pC$ for the resultant electric charge modulus propelled instantaneously from the air around a given sharp point.

To support the experimental interval found, we model the sharp point as a simple small spherical conductor of estimated radius $\tilde{r} \approx 0.1\, mm$, with electric field modulus on it surface given by

$$E = \frac{q}{4\pi\epsilon_0 \tilde{r}^2}, \tag{5}$$

and $\epsilon_0 = 8.85 \times 10^{-12} C^2/N.m^2$ the vacuum electric permittivity. Imposing again the limit $E > 3 \times 10^6\, V/m$, for the electric field generated near sharp point, we obtain $q_{theory} > 3.3\, pC$ for the lower bound of theoretical charge induced, that agrees with experimental interval found.

5 Conclusions

In this paper, we bring a semi-quantitative low-cost experiment, combining video analysis and mathematical modeling, to discuss the electrical phenomenon of the power of sharp points directed to the undergraduate classes. We developed an analytical model which shows a possibility to describe the

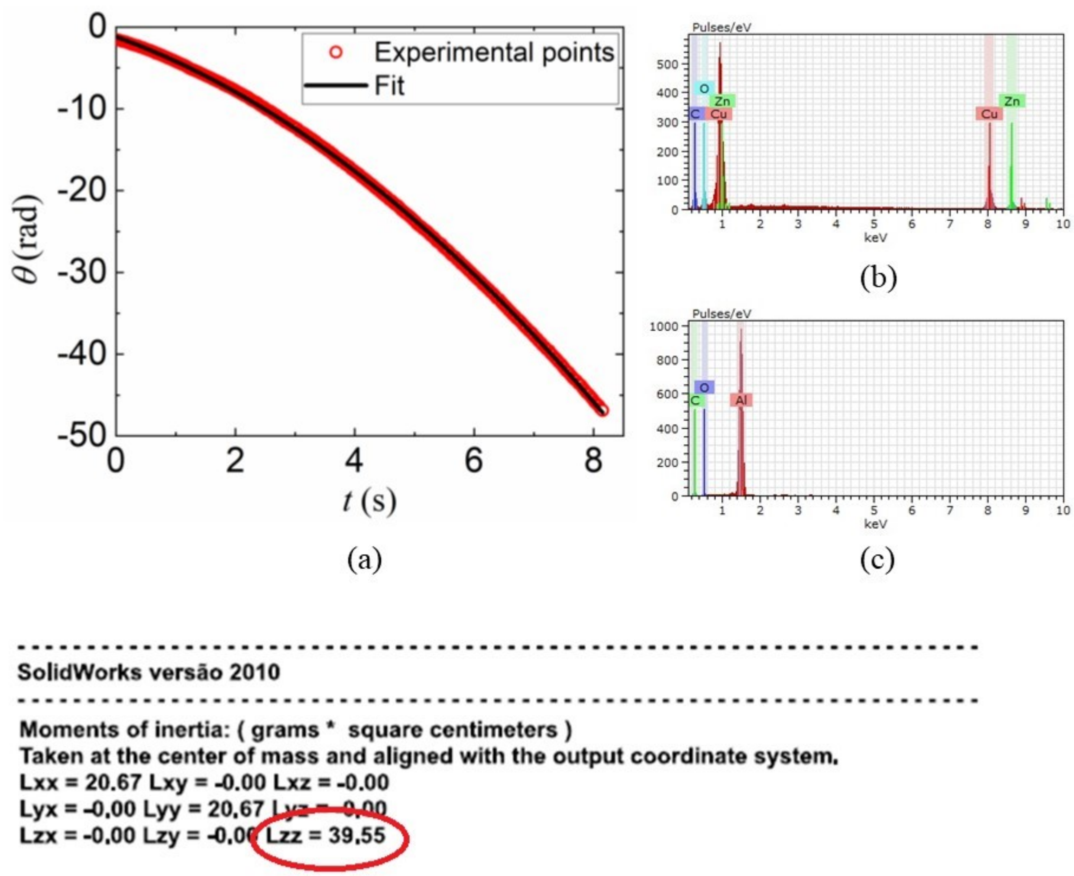

(d)

Figure 4: Output results. (a) *Tracker* fitting process of the sharp point angular position θ as a function of time t. (b) and (c) Spectra obtained, respectively, from the arm and core analysis using electronic microscopy technique. (d) *SolidWorks* output.

inertia moment of an electric whirl in terms of known and simple regular geometric solids. The model has been validated by *SolidWorks* simulations and, experimentally, using electronic microscopy, obtaining small relative percentual errors concerning the expected quantities. In the end, combining kinematics, video analysis, and rotation dynamic, we estimate a superior bound for the modulus of the electric charge propelled from the air on each instant of time, considering a simple model in which the charges are continuously emitted. This paper exposes the importance of discussing in classes how physical modeling is thought, developed, and tested using experiments and numerical simulations, also allowing the students to think about the limitations and validity of physical theories.

References

[1] J. Lavonen, K. Juuti, M. Aksela and V. Meisalo,"A professional development project for improving the use of information and communication technologies in science teaching," Technology, pedagogy and education, **15**(2), 159-174, (2006).

[2] A. M. Suduc, M. Bîzoi, G. Gorghiu and L. M. Gorghiu, "Information and communication technologies in science education," Procedia-Social and Behavioral Sciences, **15**, 1076-1080, (2011).

[3] K. Santi, S. M. Sholeh, F. Alatas, H. Rahmayanti, I. Z. Ichsan and M. M. Rahman, "STEAM in environment and science education: Analysis and bibliometric mapping of the research literature (2013-2020)," Journal of Physics: Conference Series, 012097, (2021).

[4] N. Soroko and L. Mykhailenko, "Teachers' digital competence development as an important factor for the creation and support of the STEAM-based educational environment," Studies in comparative education, (2), 47-58, (2019).

[5] S. S. Lee, "Research on The Developmental Aspects of The Steam Education Program Development in Korea," Journal of Engineering Education Transformations, **34**(2), 33-44, (2020).

[6] C. Kexel, M. Mälzer and J. Moll, "Connecting physics to ICT: demonstrating a 'Data Drawbridge'by means of guided ultrasound waves," European Journal of Physics, **39**(5), 055806, (2018).

[7] P. Klein, S. Gröber, J. Kuhn and A. Müller, "Video analysis of projectile motion using tablet computers as experimental tools," Physics Education, **49**(1), 37, (2014).

[8] W. P. N. dos Reis, D. P. Rodrigues, I. L. Rocha, R. S. Dutra and P. V. S. Souza. "An Arduino-based experiment designed to estimate the heat capacity of a nichrome resistor," Physics Education, **56**(1), 013005, (2020).

[9] I. S. Araujo, E. A. Veit and M. A. Moreira, "Physics students' performance using computational modelling activities to improve kinematics graphs interpretation," Computers Education, **50**(4), 1128-1140, (2008).

[10] T. Martins, V. L. B. de Jesus and D. G. G. Sasaki, "The Magnus effect in volleyball service by video analysis," European Journal of Physics, **43**(1), 015002, (2021).

[11] A. Jimoyiannis and V. Komis, "Computer simulations in physics teaching and learning: a case study on students' understanding of trajectory motion," Computers education, **36**(2), 183-204, (2001).

[12] E. A. Lima, R. S. Dutra and P. V. S. Souza, "Studying the Oobleck with video-analysis," Physics Education, **55**(4), 045021, (2020).

[13] V. L. B. Jesus and D. G. G. Sasaki, "A simple experiment to determine the moments of inertia of the fidget spinner by video analysis," The Physics Teacher, **56**(9), 639-642, (2018).

[14] M. Kouh, D. Holz, A. Kawam and M. Lamont, "Wiimote experiments: circular motion," The Physics Teacher, **51**(3), 146-148, (2013).

[15] S. Phommarach, P. Wattanakasiwich and I. Johnston, "Video analysis of rolling cylinders," Physics Education, **47**(2), 189, (2012).

[16] R. J. Beichner, "The impact of video motion analysis on kinematics graph interpretation skills," American Journal of physics, **64**(10), 1272-1277, (1996).

[17] J. C. C. Palacio, L. V. Abad, M. H. Giménez and J. A. Monsoriu, "Using a mobile phone acceleration sensor in physics experiments on free and damped harmonic oscillations,". American Journal of Physics, **81**(6), 472-475, (2013).

[18] H. D. Young, R. A. Freedman and A. L. Ford, Sears and Zemansky's, *University Physics*, (Vol. 3, Pearson education, 2006).

[19] J. A. Daffron and T. B. Greenslade Jr, "The Electric Whirl in the 19th and 21st Centuries. The Physics Teacher," **50**(9), 536-536, (2012).

[20] A. Michaud, "The Corona Effect," International Journal of Engineering Research and Development, e-ISSN, 01-09, (2013).

[21] P. B. Ferdinand and E. Russell Johnston, Jr, *Vector Mechanics for Engineers*, (fourth ed. McGraw-Hill, ISBN 0-07-004389-2, 1984).

[22] J. Kuo, *Electron microscopy: methods and protocols*, (Vol. 369, Springer Science Business Media, 2007).

[23] M. S. Moghaddam, R. Parvizi, M. Haddad-Sabzevar and A. Davoodi, "Microstructural and mechanical properties of friction stir welded Cu–30Zn brass alloy at various feed speeds: Influence of stir bands," Materials Design, **32**(5), 2749-2755, (2011).